John von Neumann Institute for Computing

Phase Transitions in Disordered Ferromagnets

Wolfhard Janke, Pierre-Emmanuel Berche, Christophe Chatelain, Bertrand Berche

published in

NIC Symposium 2004, Proceedings,
Dietrich Wolf, Gernot Münster, Manfred Kremer (Editors),
John von Neumann Institute for Computing, Jülich,
NIC Series, Vol. **20**, ISBN 3-00-012372-5, pp. 241-250, 2003.

http://www.fz-juelich.de/nic-series/volume20

Phase Transitions in Disordered Ferromagnets

Wolfhard Janke[1] **, Pierre-Emmanuel Berche**[2] **, Christophe Chatelain**[1,3]**, and Bertrand Berche**[3]

[1] Institut für Theoretische Physik, Universität Leipzig
Augustusplatz 10/11, 04109 Leipzig, Germany
E-mail: {wolfhard.janke, christophe.chatelain,}@itp.uni-leipzig.de

[2] Groupe de Physique des Matériaux, Université de Rouen
76821 Mont Saint-Aignan Cedex, France
E-mail: pierre.berche@univ-rouen.fr

[3] Laboratoire de Physique des Matériaux, Université Henri Poincaré,
Nancy I, BP 239, 54506 Vandœuvre les Nancy Cedex, France
E-mail: {chatelai, berche}@lpm.u-nancy.fr

We review recent large-scale Monte Carlo simulations of the three-dimensional q-state Potts ferromagnet with $q = 2$ and 4 subject to quenched, random bond dilution. For the Ising model ($q = 2$) both finite-size and temperature scaling are investigated in order to estimate the critical exponents associated with the disorder fixed point and to elucidate the cross-over between pure, disorder and percolation critical behaviour. For the 4-state Potts model the rather strong first-order phase transition of the pure system is found to persist for small dilutions, whereas for larger dilutions the theoretically expected softening to a continuous transition is confirmed and quantified. The properties of the underlying disorder distributions of thermal observables are discussed and illustrated with a few selected examples.

1 Introduction

Experiments on phase transitions in magnetic materials are usually subject to randomly distributed impurities. At continuous phase transitions, depending on the temperature resolution and the concentration of the impurities, the disorder may significantly influence measurements of critical exponents[1]. To emphasize this effect, in some experiments[2] non-magnetic impurities are introduced in a controlled way; see Fig. 1 for an example. Since the mobility of impurities is usually much smaller than the typical time scale of spin fluctuations, one may model the disorder effects in a completely "frozen", so-called "quenched" approximation. This limit is opposite to "annealed" disorder which refers to the case where the two relevant time scales are of the same order.

With the additional assumption that the quenched, randomly distributed impurities are completely uncorrelated, Harris[3] showed a long time ago under which conditions a *continuous* transition of an idealised pure material is modified by disorder coupling to the energy of the system. Another interesting case are random fields[4] coupling to the order parameter which we shall not, however, consider here. According to this so-called Harris criterion, the critical behaviour of the pure system around the transition temperature T_c is stable against quenched disorder when the critical exponent $\alpha_{\rm pure}$ of the specific heat, $C \propto |T - T_c|^{-\alpha_{\rm pure}}$, is negative. In renormalization-group language the perturbation is then "irrelevant" and the values of all critical exponents $\alpha, \beta, \gamma, \ldots$ remain unchanged. On the other hand, when $\alpha_{\rm pure} > 0$, then quenched disorder should be "relevant" and the

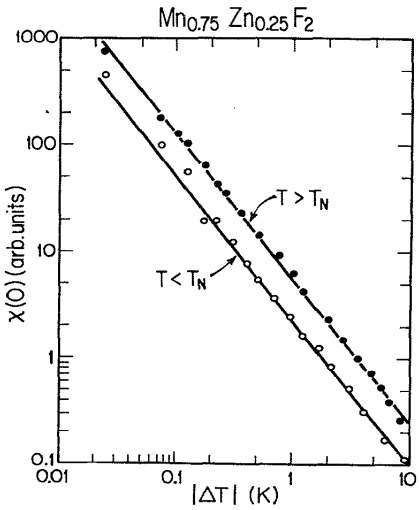

Figure 1. Neutron scattering measurements of the susceptibility in $\mathrm{Mn_{0.75}Zn_{0.25}F_2}$ close to criticality, governed by the disorder fixed point of the Ising model over the reduced temperature interval $4 \times 10^{-4} < |T/T_c - 1| < 2 \times 10^{-1}$. The solid lines show power-law fits with exponent $\gamma = 1.364(76)$ above and below T_c (after Mitchell *et al.*[2]).

renormalization-group flow approaches a new disorder fixed point governed by altered critical exponents. An example is the three-dimensional (3D) Ising model universality class with $\alpha_{\rm pure} \approx 0.110 > 0$. The intermediate situation $\alpha_{\rm pure} = 0$ is a special, "marginal" case where no easy predictions can be made. A typical example for the latter situation is the two-dimensional (2D) Ising model where quenched disorder is known to generate logarithmic modifications.

If the pure system exhibits a *first-order* phase transition, quenched disorder always leads to a softening effect and may even turn the transition into a continuous one[5]. In two dimensions this is always the case, independent of the concentration ("strength") of the disorder[6]. In three (and higher) dimensions, on the other hand, the concentration of disorder does matter and at a finite concentration a tricritical point may be observed which separates "non-softened" first-order and "softened" second-order regimes[7,8].

In 2D the scenarios sketched above have been confirmed experimentally for many different materials, and also for simple lattice models by a variety of different theoretical methodologies, including field theoretic renormalization-group analyses, transfer-matrix studies, high-temperature series expansions and Monte Carlo simulations, to mention the most important ones[9]. In 3D an experimental verification of the qualitative influence of disorder is shown in Fig. 1 where the measured critical exponent $\gamma = 1.364(76)$ of the susceptibility $\chi \propto |T - T_c|^{-\gamma}$ is clearly different from that of the pure 3D Ising model, $\gamma_{\rm pure} = 1.2396(13)$. Theoretical results, on the other hand, remained relatively scarce in 3D until recently. Most analytical renormalization group and computer simulation studies focused on the Ising model[10,11], usually assuming *site* dilution when working numerically. Only quite recently the *site*-diluted 3-state Potts model[12], which exhibits a first-order phase transition in the pure case, has been added to this short list.

This motivated us to set up a systematic Monte Carlo (MC) computer simulation study of the 3D 4-state Potts model with *bond* dilution[13,14]. Since the pure model's first-order transition is much stronger than that of the 3-state model studied in Ref. 12, we expected that our choice would lead to a much more conclusive characterisation of the tricritical point. For a better overview and to gauge our simulation tools we also considered the 3D 2-state (Ising) model, again with *bond* dilution[15]. Modelling the disorder by bond dilution enabled us to test the expected universality with respect to the type of disorder distribution and in addition facilitates for both models a quantitative comparison with recent high-temperature series expansions[16,17].

The remainder of this mini-review is organised as follows. In Sec. 2 we define the models considered and briefly describe the simulation setup. Section 3 is devoted to a summary of our results, first for the Ising and then for the 4-state Potts model. Finally, in Sec. 4 we close with our conclusions.

2 Model and Simulation Setup

The 3D bond-diluted q-state Potts model is defined by the Hamiltonian

$$H = -\sum_{\langle ij \rangle} J_{ij} \delta_{\sigma_i,\sigma_j} \ , \quad \sigma_i = 1, \ldots, q \ , \tag{1}$$

where the sum extends over all nearest-neighbour pairs of a cubic lattice of size L^3 with periodic boundary conditions, and the couplings J_{ij} are distributed according to the distribution

$$\wp(J_{ij}) = p\delta(J_{ij} - J) + (1-p)\delta(J_{ij}) \ . \tag{2}$$

The dilution parameter p is thus the concentration of magnetic bonds in the system, i.e., $p = 1$ corresponds to the pure case. Below the percolation threshold[18] $p_c = 0.248\,812\,6(5)$ one does not expect any finite-temperature phase transition since without a percolating (infinite) cluster of spins long-range order cannot develop.

The model (1), (2) was studied by means of large-scale MC simulations using the Swendsen-Wang (SW) cluster algorithm[19] in the regime of second-order transitions, and multibondic simulations[20–22] in the regime where the first-order transition of the pure 4-state Potts model persists, i.e., at weak dilutions close to $p = 1$. To arrive at final results, for each dilution, temperature and lattice size, the MC estimates $\langle Q_{\{J\}} \rangle$ of thermodynamic quantities $Q_{\{J\}}$ for a given random distribution $\{J\}$ of diluted bonds have to be averaged over many different disorder realisations,

$$Q \equiv [\langle Q_{\{J\}} \rangle]_{\rm av} = \frac{1}{\#\{J\}} \sum_{\{J\}} \langle Q_{\{J\}} \rangle \ , \tag{3}$$

where $\#\{J\}$ is the number of realisations considered. Denoting the empirically determined distribution of $\langle Q_{\{J\}} \rangle$ by $\mathcal{P}(\langle Q_{\{J\}} \rangle)$, this so-called quenched average can also be obtained from

$$Q = \int \mathcal{D}J_{ij} \wp(J_{ij}) \langle Q_{\{J\}} \rangle = \int d\langle Q_{\{J\}} \rangle \mathcal{P}(\langle Q_{\{J\}} \rangle) \langle Q_{\{J\}} \rangle \ , \tag{4}$$

where a discretized evaluation of the integrals for finite $\#\{J\}$ is implicitly implied. While conceptually straightforward, the quenched average in (3) is computationally very demanding since the number of realisations $\#\{J\}$ usually must be large, often of the order of a few thousands. In fact, if this number is chosen too small one may observe *typical* rather than average values[23] which may differ significantly when the distribution $\mathcal{P}(\langle Q_{\{J\}}\rangle)$ exhibits a long tail (which in general is hard to predict beforehand).

3 Results

3.1 3D Bond-Diluted Ising Model

Let us first discuss the Ising model where for all dilutions above p_c second-order phase transitions are expected. To get a rough overview of the dependence of the susceptibility peaks on the dilution, we first performed for $p = 0.95, 0.90, \ldots, 0.36$ and moderate system sizes SW cluster MC simulations with $N_{\mathrm{MCS}} = 2\,500$ MC sweeps (MCS) each. By performing quite elaborate analyses of autocorrelation times, this statistics was judged to be reasonable ($N_{\mathrm{MCS}} > 250\ \tau_e$). By applying histogram reweighting to each disorder realisation and then averaging the curves over $2\,500 - 5\,000$ realisations we finally arrived at the data shown in Fig. 2. From the locations of the maxima we derived the phase diagram of the model in the $p - T$ plane which turned out to be in excellent agreement with a single-bond effective-medium (EM) approximation[24],

$$K_c^{\mathrm{EM}}(p) = \ln\left[\frac{(1-p_c)e^{K_c(1)} - (1-p)}{p - p_c}\right] , \tag{5}$$

where $K_c(1) = J/k_BT_c(1) = 0.443\,308\,8(6)$ is the precisely known transition point of the pure 3D Ising model[25], so we can refrain from reproducing it here. As an independent confirmation of (5), the phase diagram also coincides extremely well with recent results from high-temperature series expansions[16].

The quality of the disorder averages was judged by looking at the distributions $\mathcal{P}(\chi_{\{J\}})$ and computing running averages over the number of realisations taken into account. As can

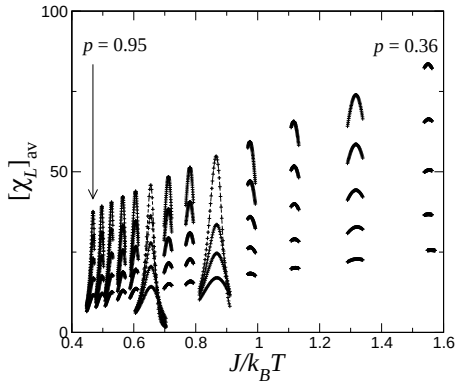

Figure 2. The average magnetic susceptibility $[\chi_L]_{\mathrm{av}}$ of the 3D bond-diluted Ising model versus $K = J/k_BT$ for several concentrations p and $L = 8, 10, 12, 14, 16, 18$, and 20. For each value of p and each lattice size L, the curves are obtained by standard histogram reweighting of the simulation data at one value of K.

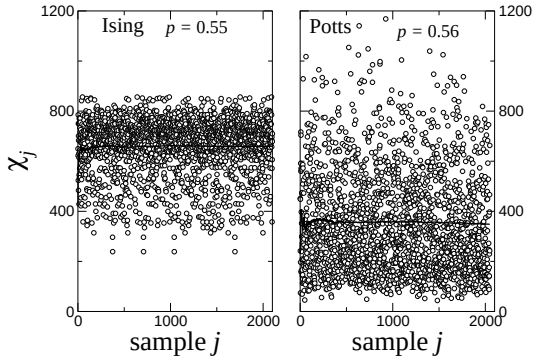

Figure 3. Disorder distribution of the susceptibility for the 3D Ising and 4-state Potts model with a concentration of magnetic bonds of 0.55 and 0.56, respectively, at $K_c(L)$ ($= 0.8649$ resp. 1.12945) for $L = 64$. In the latter case, the concentration $p = 0.56$ belongs to the second-order regime. The running average over the samples is shown by the black line.

be seen in Fig. 3, the dispersion of the values of $\chi_{\{J\}}$ is not very large and the fluctuations in the running average disappear already after a few hundreds of realisations.

In order to study the critical behaviour in more detail, we concentrated on the three particular dilutions $p = 0.7$, 0.55, and 0.4. In a first set of simulations we focused on the finite-size scaling (FSS) behaviour for lattice sizes up to $L = 96$. From previous FSS studies it is known that ratios of critical exponents are very similar for the pure and disordered model, e.g., $\gamma/\nu = 1.966(6)$ (pure[26]) and $\gamma/\nu = 1.963(5)$ (disordered[27]). The only distinguishing quantity is the correlation length exponent ν which can be extracted, e.g., from the derivative of the magnetisation versus inverse temperature, $[d \ln m/dK]_{\rm av} \propto L^{1/\nu}$, at K_c or the locations of the susceptibility maxima. Using the latter unbiased option and performing least-square fits including data from $L_{\rm min}$ to $L_{\rm max} = 96$ we obtained the effective critical exponents shown in Fig. 4. For the dilution closest to the pure model ($p = 0.7$), the system is influenced by the pure fixed point with $1/\nu = 1.5863(33)$. On the other hand, when the bond concentration is small ($p = 0.4$), the vicinity of the percolation fixed point where $1/\nu \approx 1.12$ induces a decrease of $1/\nu$ below its expected disorder value. The dilution for which the cross-over effects are the least is around $p = 0.55$ which suggests that the scaling corrections should be rather small for this specific dilution. For the exponents ratios we obtained $\beta/\nu = 0.515(5), 0.513(5)$, and $0.510(5)$, and $\gamma/\nu = 1.965(10), 1.977(10)$, and $2.000(10)$, for $p = 0.7, 0.55$, and 0.4, respectively.

The main problem of the FSS study is the competition between different fixed points (pure, disorder, percolation) in combination with corrections-to-scaling terms $\propto L^{-\omega}$, which we found hard to control for bond dilution. In contrast to recent claims for the site-diluted model that $\omega \approx 0.4$, we were not able to extract a reliable estimate of ω from our data.

In the second set of simulations we examined the temperature scaling of the magnetisation and susceptibility for lattice sizes up to $L = 40$. From this data one can directly extract the exponents β and γ whose relative deviation from the pure model is comparable to that of ν, e.g. $\gamma = 1.2396(13)$ (pure[26]) and $\gamma = 1.342(10)$ (disordered[27]). The results for the susceptibility and $p = 0.7$ are shown in Fig. 5. We see that for the greatest

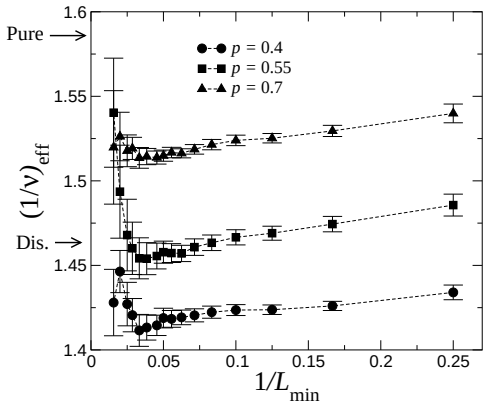

Figure 4. Effective exponents $(1/\nu)_{\rm eff}$ as a function of $1/L_{\rm min}$ for $p = 0.4$, 0.55, and 0.7.

sizes, the effective critical exponent $\gamma_{\rm eff}(|t|) = -d\ln[\chi]_{\rm av}/d\ln|t|$ is stable around 1.34 when $|t| = |K - K_c|$ is not too small, i.e., when the finite-size effects are not too strong. The plot of $\gamma_{\rm eff}(|t|)$ vs. the rescaled variable $L^{1/\nu}|t|$ shows that the critical power-law behaviour holds in different temperature ranges for the different sizes studied. As expected, the size-effects are more sensitive when the lattice size is small and the critical behaviour is better described when the size increases.

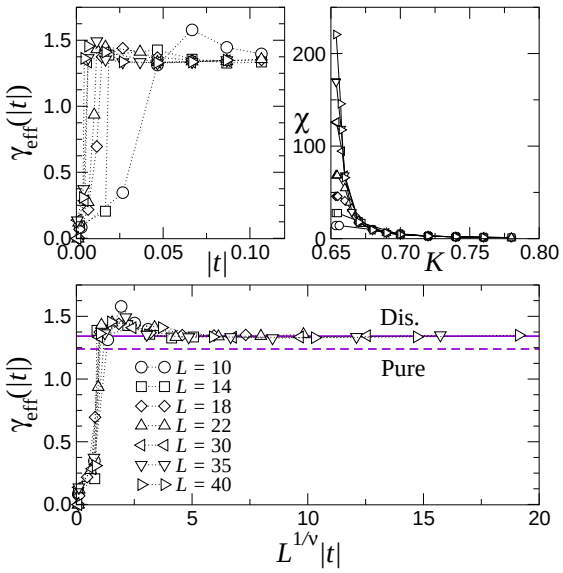

Figure 5. Variation of the temperature dependent effective critical exponent $\gamma_{\rm eff}(|t|) = -d\ln[\chi]_{\rm av}/d\ln|t|$ in the low-temperature phase of the 3D bond-diluted Ising model for $p = 0.7$ and several lattice sizes $L = 10,\ 14,\ 18,\ 22,\ 30,\ 35,\ 40$ as a function of the reduced temperature $|t|$ (top left) and $L^{1/\nu}|t|$ (bottom). The horizontal dashed and solid lines indicate the pure and site-diluted values of γ. The susceptibility vs. the coupling strength $K = J/k_BT$ in the ordered phase is shown in the upper right plot.

3.2 3D Bond-Diluted 4-State Potts Model

Let us now turn to the 4-state Potts model which exhibits a rather strong first-order phase transition in the pure case. In order to map out the phase diagram of the diluted model we considered all concentrations p in the interval $[0.28, 1]$ in steps of 0.04 and determined again the locations of the maxima of the susceptibility for a given lattice size L. The resulting phase diagram is again in very good agreement with the effective-medium approximation (5), here with[13] $K_c(1) = 0.62863(2)$, and estimates from high-temperature series expansions[17].

In a second step, the order of the phase transitions was investigated. To satisfy our criterion $N_{\rm MCS} > 250\ \tau_e$, here the number of MC sweeps had to be increased to much larger values (up to $15\,000 - 30\,000$) than in the Ising case. In fact, a first indication for a crossover between first- and second-order transitions with decreasing dilution p could be derived from the autocorrelation times. In the first-order regime we performed multibondic simulations[20] and estimated the interface tension from

$$\sigma_{od} = \frac{1}{2L^2} \log \frac{P_{\rm max}}{P_{\rm min}} \ , \tag{6}$$

where $P_{\rm max}$ is the maximum of the probability density reweighted to the temperature where the two peaks are of equal height, and $P_{\rm min}$ is the minimum in between, see Fig. 6. The linear extrapolations of σ_{od} in $1/L$ in the lower part of Fig. 6 imply non-vanishing interface tensions only for $p = 0.84$ and above. For $p \leq 0.76$, σ_{od} seems to vanish in the infinite-volume limit, being indicative of the expected softening to a second-order phase transition. The tricritical point would thus be located around $p = 0.76 - 0.84$, in good agreement with

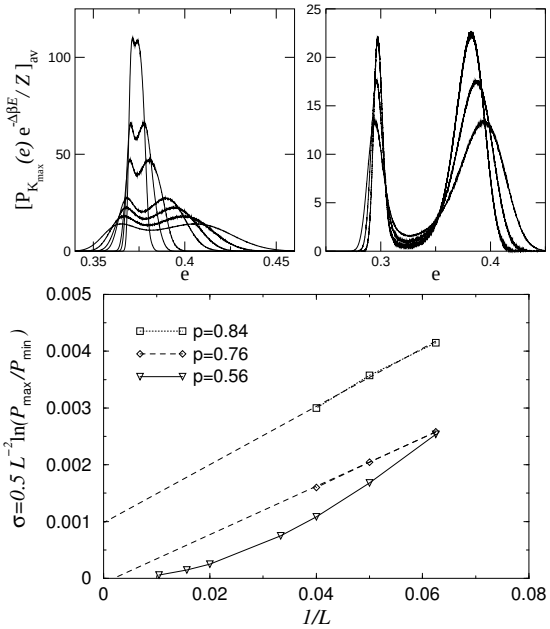

Figure 6. Probability density of the energy of the 3D bond-diluted 4-state Potts model reweighted to equal peak height for $p = 0.56$ (top left) and $p = 0.84$ (top right). Interface tension versus inverse lattice size (bottom).

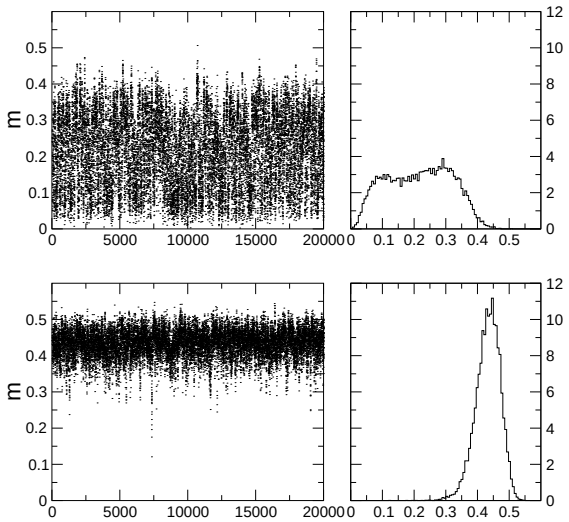

Figure 7. Time series and histogram of the magnetisation at $p = 0.36$ ($L = 16$). The upper part shows the time evolution for a rare event with high susceptibility and the lower one a typical event where the magnetisation fluctuations are reduced. On the right part the resulting (thermal) probability distributions are shown.

the estimate of $p = 0.80$ derived from our analysis of autocorrelation times.

Below this concentration, the system exhibits a second-order transition. This can be illustrated qualitatively by typical single-peak order-parameter probability distributions at the transition temperature as shown in Fig. 7. To confirm the softening to second-order phase transitions for $p \leq 0.76$ we performed a detailed FSS[13] study at $p = 0.56$ with lattice sizes ranging up to $L = 96$ and the number of realisations varying between 2 000 and 5 000. As can be inspected in Fig. 3, the variance of the $\chi_{\{J\}}$ measurements is somewhat larger than in the Ising model and the distribution exhibits a long tail towards large susceptibilities, reflecting the first-order like signal of a few rare-events such as that shown in the upper part of Fig. 7.

The choice of $p = 0.56$ is motivated by our observation that in this range of dilutions the corrections to asymptotic FSS of the effective transition points are minimal. The log-log plot for $[\chi]_{\mathrm{av,max}}$ in Fig. 8 indeed suggests that for this quantity the corrections become quite small above $L = 30$, and fits of the form $a_\chi L^{\gamma/\nu}$ starting at $L_{\min} > 30$ yield $\gamma/\nu = 1.50(2)$. Using the data for $L < 30$ only, on the other hand, we obtained perfect fits assuming percolation exponents[18], $\gamma/\nu \approx 2.05$, cf. Fig. 8. Similarly, the FSS of the quantity $[(d \ln m/dK)_{K_{\max}}]_{\mathrm{av}} \propto L^{1/\nu}$ gives for $L_{\min} > 30$ an estimate of the exponent $1/\nu = 1.33(3)$, consistent with the stability condition[28] $1/\nu \leq D/2 = 1.5$ at the disorder fixed point. The same procedure was applied to the magnetisation $[m_{K_{\max}}]_{\mathrm{av}} \propto L^{-\beta/\nu}$, but here the associated critical exponent turned out to be not yet stable. We therefore also considered the FSS behaviour of higher (thermal) moments of the magnetisation, $[\langle \mu^n \rangle]_{\mathrm{av}}$, which should scale with an exponent $n\beta/\nu$. The results for the first moments exhibit, however, again much stronger corrections to scaling than we observed for $[\chi]_{\mathrm{av}}$ or $[d \ln m/dK]_{\mathrm{av}}$, leading to quite a conservative final estimate of $\beta/\nu = 0.65(5)$. We never-

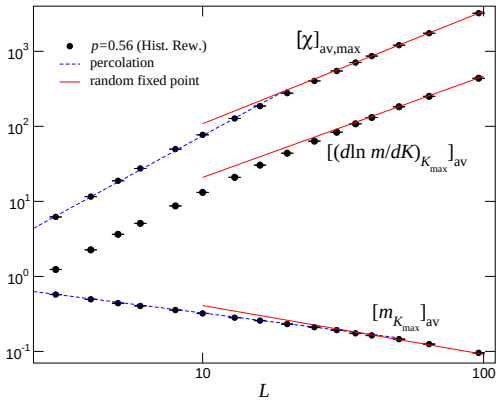

Figure 8. FSS behaviour of the susceptibility, $[d\ln m/dK]_{\rm av}$, and magnetisation at $K_{\rm max}$ for the 3D bond-diluted 4-state Potts model at $p = 0.56$ (with vertical offsets added for the sake of clarity). The scaling behaviour for small lattice sizes below a crossover length scale is presumably governed by the percolation fixed point.

theless note that our results do not fit satisfactorily the hyperscaling law $2\beta/\nu = D - \gamma/\nu$. The reason could be strong corrections-to-scaling at the disorder fixed point which are hard to cope with for medium-sized systems[13].

4 Conclusions

By performing large-scale Monte Carlo simulations we have investigated the influence of bond dilution on the critical properties of the 3D Ising and 4-state Potts models. In the 3D Ising case the universality class of the disordered model is modified by disorder but its precise characterisation turned out be difficult because of the competition between the different fixed points which induce crossover effects, even for relatively large lattice sizes.

Applying similar techniques to the 3D 4-state Potts model we obtained clear evidence for softening to a continuous transition at strong disorder, with estimates for the critical exponents of $\nu = 0.752(14)$, $\gamma = 1.13(4)$, and $\beta = 0.49(5)$ at $p = 0.56$. The analysis of both the autocorrelation time and the interface tension leads to the conclusion of a tricritical point around $p = 0.80$.

Acknowledgements

We thank Meik Hellmund and Loic Turban for helpful discussions. This work was partially supported by the PROCOPE exchange programme of DAAD and EGIDE, the EU-Network HPRN-CT-1999-000161 "EUROGRID: *Discrete Random Geometries: From solid state physics to quantum gravity*", the DFG under grant No. JA 483/17, and the German-Israel-Foundation (GIF) under grant No. I-653-181.14/1999. We gratefully acknowledge the computer-time grants hlz061 of NIC, Jülich, h0611 of LRZ, München, 062 0011 of CINES, Montpellier, and 2000007 of CRIHAN, Rouen, which were essential for this project.

References

1. J. Cardy, *Scaling and Renormalization in Statistical Physics* (Cambridge University Press, Cambridge, 1996), Chap. 8.
2. P.W. Mitchell, R.A. Cowley, H. Yoshizawa, P. Böni, Y.J. Uemura, and R.J. Birgeneau, Phys. Rev. B **34**, 4719 (1986).
3. A.B. Harris, J. Phys. C **7**, 1671 (1974).
4. A.P. Young (ed.), *Spin Glasses and Random Fields* (World Scientific, Singapore, 1998).
5. Y. Imry and M. Wortis, Phys. Rev. B **19**, 3580 (1979).
6. M. Aizenman and J. Wehr, Phys. Rev. Lett. **62**, 2503 (1989).
7. J. Cardy and J.L. Jacobsen, Phys. Rev. Lett. **79**, 4063 (1997).
8. For a review, see J. Cardy, Physica A **263**, 215 (1999).
9. S. Chen, A.M. Ferrenberg, and D.P. Landau, Phys. Rev. E **52**, 1377 (1995); C. Chatelain and B. Berche, Phys. Rev. Lett. **80**, 1670 (1998); T. Olson and A.P. Young, Phys. Rev. B **60**, 3428 (1999); for a review, see B. Berche and C. Chatelain, cond-mat/0207421, to appear in: *Order, Disorder and Criticality*, ed. Y. Holovatch (World Scientific, Singapore, 2003) (in print).
10. W. Selke, L.N. Shchur, and A.L. Talapov, in: D. Stauffer (ed.), *Annual Reviews of Computational Physics I* (World Scientific, Singapore, 1994), pp. 17–54.
11. For a recent overview, see R. Folk, Y. Holovatch, and T. Yavors'kii, Physics Uspiekhi **173**, 175 (2003) [e-print cond-mat/0106468].
12. H.G. Ballesteros, L.A. Fernández, V. Martín-Mayor, A. Muñoz Sudupe, G. Parisi, and J.J. Ruiz-Lorenzo, Phys. Rev. B **61**, 3215 (2000).
13. C. Chatelain, B. Berche, W. Janke, and P.-E. Berche, Phys. Rev. E **64**, 036120 (2001).
14. C. Chatelain, P.-E. Berche, B. Berche, and W. Janke, Nucl. Phys. B (Proc. Suppl.) **106&107**, 899 (2002); Comp. Phys. Comm. **147**, 431 (2002).
15. P.-E. Berche, C. Chatelain, B. Berche, and W. Janke, Comp. Phys. Comm. **147**, 427 (2002).
16. M. Hellmund and W. Janke, Comp. Phys. Comm. **147**, 435 (2002).
17. M. Hellmund and W. Janke, Nucl. Phys. B (Proc. Suppl.) **106&107**, 923 (2002); Phys. Rev. E **67**, 026118 (2003).
18. C.D. Lorenz and R.M. Ziff, Phys. Rev. E **57**, 230 (1998).
19. R.H. Swendsen and J.S. Wang, Phys. Rev. Lett. **58**, 86 (1987).
20. W. Janke and S. Kappler, Phys. Rev. Lett. **74**, 212 (1995); M.S. Carroll, W. Janke, and S. Kappler, J. Stat. Phys. **90**, 1277 (1998).
21. B.A. Berg, Fields Inst. Commun. **26**, 1 (2000).
22. W. Janke, Physica A **254**, 164 (1998).
23. B. Derrida, Phys. Rep. **103**, 29 (1984); A. Aharony and A.B. Harris, Phys. Rev. Lett. **77**, 3700 (1996); S. Wiseman and E. Domany, Phys. Rev. Lett. **81**, 22 (1998).
24. L . Turban, Phys. Lett. A **75**, 307 (1980); J. Phys. C **13**, L13 (1980).
25. A.L. Talapov and H.W.J. Blöte, J. Phys. A **29**, 5727 (1996).
26. R. Guida and J. Zinn-Justin, J. Phys. A **31**, 8103 (1998).
27. H.G. Ballesteros, L.A. Fernández, V. Martín-Mayor, A. Muñoz Sudupe, G. Parisi, and J.J. Ruiz-Lorenzo, Phys. Rev. B **58**, 2740 (1998).
28. J.T. Chayes, L. Chayes, D.S. Fisher, and T. Spencer, Phys. Rev. Lett. **57**, 2999 (1986).